1 SUPPORTING INFORMATION

Table S1 Plant parameters of ModEST.

Parameter	Unit	Description	PFT 1	PFT 2	PFT 3	PFT 4	PFT 5	PFT 6	Source
Phenology	-	Evergreen (E) or raingreen (R) phenology	E	E	E	R	E	E	Kattge et al., (2020)
T_1	°C	Lowest temperature limit for photosynthesis	-4	-4	-4	-4	-4	-4	Sitch et al., (2000), temperate needle/broad-leaved evergreen species
T_2	°C	Lower temperature limit for optimal photosynthesis	20	20	20	20	20	20	Sitch et al., (2000), temperate needle/broad-leaved evergreen species
T_3	°C	Higher temperature limit for optimal photosynthesis	30	30	30	30	30	30	Sitch et al., (2000), temperate needle/broad-leaved evergreen species
T_4	°C	Highest temperature limit for photosynthesis	42	42	42	42	42	42	Sitch et al., (2000), temperate needle/broad-leaved evergreen species
SLA	$m^2\ kg^{-1}$	Specific leaf area	12.421	4.7766	8.082	14.704	5.6	2.612	Kattge et al., (2020)
g_{min}	$mm\ s^{-1}$	Minimum canopy conductance that occurs due to processes other than photosynthesis	0.5	0.3	0.3	0.5	0.3	0.3	Kattge et al., (2020) for leaf area clustered into two groups (needle versus broad leaved) and parameter value from Sitch et al., (2000) for broad-leaved (0.5) and needle-leaved (0.3) plants
CN_{leaf}	-	Carbon to nitrogen ratio of the leaves	44.0	94.01	51.87	44.68	97.62	161.87	Kattge et al., (2020)
CN_{sap}	-	Carbon to nitrogen ratio of the sapwood	100.76	142.43	109.79	101.6	144.49	172.25	Correlation with C:N in leaves from Kattge et al., (2020) and equations from measured data in Perring et al., (2012) and Fiedler et al., (unpublished)
CN_{root}	-	Carbon to nitrogen ratio of the roots	75.94	101.61	81.5	76.46	102.88	119.98	Correlation with C:N in leaves from Kattge et al., (2020) and equations from measured data in Perring et al., (2012) and Fiedler et al., (unpublished)
k_{store}	-	Constant for maximum N storage	0.05	0.05	0.05	0.15	0.05	0.05	Kattge et al., (2020) for phenology and parameter values from Smith et al., (2014) for evergreen (0.05) and deciduous plants (0.15)
$root_{L1}$	-	Fraction of roots between 0-50cm of the soil horizon	0.69	0.87	0.65	0.77	0.64	0.45	Kattge et al., (2020)
$root_{L2}$	-	Fraction of roots between 50-150cm of the soil horizon	0.31	0.13	0.35	0.23	0.36	0.55	Kattge et al., (2020)
$CN_{leaf,min}$	-	Minimum bound of C:N in the leaves	29.1	46.8	13.9	19.8	40.5	34.5	Kattge et al., (2020)
$CN_{leaf,max}$	-	Maximum bound of C:N in the leaves	34.7	58.6	20.9	21	61.4	38.9	Kattge et al., (2020)

Parameter	Unit	Description	PFT 1	PFT 2	PFT 3	PFT 4	PFT 5	PFT 6	Source
e_{max}	mm day^{-1}	Maximum water transport capacity for transpiration	5.0	5.0	5.0	5.0	5.0	5.0	Sitch et al., (2003)
LM/RM	-	Allometric constant to transfer from leaf mass to root mass	1.0	1.0	1.0	1.0	1.0	1.0	Sitch et al., (2003)
WP	cm	Plant water potential at wilting point	23460	23460	23460	23460	23460	23460	Bartlett et al., (2012)
r_{coef}	kgC kgN^{-1} day^{-1}	Respiration coefficient that accounts for the acclimation of plant respiration rates at average ambient temperatures (10°C)	0.066	0.066	0.066	0.066	0.066	0.066	Sitch et al., (2003)
LtS	-	Allometric constant to transfer from sapwood area to leaf area	8000	8000	8000	8000	8000	8000	Sitch et al., (2003)
WD	kgC m^{-3}	Wood density	624.2	597.8	606.7	637.4	623.3	668.3	Kattge et al., (2020)
a_2	-	Parameter in allometric equation that transfers stem diameter to plant height	28.36	2.29	6.7	11.26	8.68	3.59	Kattge et al., (2020)
a_3	-	Parameter in allometric equation that transfers stem diameter to plant height	0.67	0.67	0.67	0.67	0.67	0.67	Schaphoff et al., (2018)
a_1	-	Parameter in allometric equation that transfers stem diameter to crown area	22.65	29.16	21.05	21.21	32.15	30.16	Kattge et al., (2020)
r_{rp}	-	Parameter in allometric equation that transfers stem diameter to crown area	0.51	0.72	0.53	0.46	0.46	0.5	Kattge et al., (2020)
maxCA	m^2	Maximum possible crown area	36	39	29	30	82	40	Kattge et al., (2020)
seedMass	mg	Seed mass	34.35	20.11	13.42	37.77	25.24	40.6	Kattge et al., (2020)
meanDisp	m	Mean dispersal distance	48.01	2.76	9.25	17.18	31.26	4.83	Relationship between median plant height (Kattge et al., 2020) and dispersal distance (Thomson et al., 2011)
sdDisp	m	Standard deviation of dispersal distance	2	2	2	2	2	2	assumed
p_{germ}	-	Germination probability	0.84	0.89	0.88	0.81	0.82	0.86	Kattge et al., (2020)
LAI_{ini}	-	Leaf area index of the sapling	1.5	1.5	1.5	1.5	1.5	1.5	Sitch et al., (2000)
tmort	-	Yearly relative growth above which plant dies	0.98	0.98	0.98	0.98	0.98	0.98	assumed

4

Table S2 Soil parameters of ModEST.

Parameter	Unit	Description	Clay loam	Loam	Sandy clay loam	Sandy loam	Source
S_f	mm	Effective suction	208.8	88.9	218.5	110.1	Rawls et al., (1992)
K_s	mm h^{-1}	Saturated hydraulic conductivity	4.2	3.9	2.8	55.8	Rawls et al., (1998)
fc	$m^3\ m^{-3}$	Field capacity	0.371	0.303	0.305	0.27	Rawls et al., (1992)
rw	$m^3\ m^{-3}$	Residual Water Content	0.075	0.027	0.068	0.041	Rawls et al., (1992)
$F_{L2,frac}$	-	Infiltration rate into layer 2	0.1	0.1	0.1	0.1	Tietjen et al. (2009)
$F_{L2,max}$	mm h^{-1}	Maximum total infiltration into layer 2	1.5	1.5	1.5	1.5	Rawls et al., (1992)
d	-	Constant for diffusion coefficient	0.01	0.01	0.01	0.01	Tietjen et al. (2009)
BD	$g\ cm^{-3}$	Bulk density	1.425	1.425	1.625	1.45	Rawls et al., (1992)
c_{clay}	$m^3\ m^{-3}$	Clay content	0.35	0.2	0.3	0.1	USDA 2020
n_{dep}	g ha^{-1} $year^{-1}$	Daily nitrogen deposition	4.93	4.93	4.93	4.93	Dentener et al., (2006)

S1: Identification and Parameterisation of Plant Functional Types

We determined the major PFTs that best represent the woody plant species occurring across MTEs. The focus on PFTs instead of plant species allows us to draw general conclusions on the link between plant traits and ecosystem functions for plant assemblages of Mediterranean-type regions. To our knowledge, this is the first approach classifying woody plant species occurring in MTEs in general. So far, classification has only been done for specific Mediterranean-type sites (e.g. Spain: Díaz Barradas et al., 1999; Australia: Enright et al., 2014) and mostly based on morphological traits that are not necessarily linked to biogeochemical functions (e.g. Israel: Koniak et al., 2009, 2011).

For deriving PFTs, we first acquired data pertaining to ten plant traits (Table S3) for all shrubs and tree taxa observations (515 in total) from the TRY database (Kattge et al., 2020) within the Mediterranean climate region (temperate hot dry-summer [Csa] and temperate cool dry-summer [Csb]; Köppen, 1900;

Kottek et al., 2006; Peel et al., 2007). We removed alien plant species that were found in unnatural settings (e.g. botanic gardens) within these regions. The plant traits we focused on allowed us to capture the functional diversity of Mediterranean-type plant species regarding their effects on water, nutrient and carbon cycling (Table S3). Simultaneously, these traits had a comprehensive data coverage within TRY and included leaf dry mass, leaf nitrogen, leaf area, photosynthesis rate, plant height, stomatal conductance, specific leaf area, wood density, leaf phenology, and nitrogen fixation. Replicate trait measurements for the same species and region were averaged by taking the arithmetic mean for numerical traits or the mode for categorical traits.

We then generated our representative PFTs by a cluster analysis of all selected woody species based on their trait similarities. First, numeric trait variables were centred and scaled (Stekhoven & Buhlmann, 2012). As a cluster analysis does not allow for incomplete data, we filled data gaps via additional resources (Table S3) and a nonparametric imputation based on Random Forest (package 'missForest' in R, allowing imputation of datasets containing continuous and/or categorical variables including complex interactions and nonlinear relations; Stekhoven & Buhlmann, 2012). For the cluster analysis, we first calculated a Gower distance matrix computing all pairwise trait dissimilarities between species (function 'daisy' of package 'cluster' in R; Maechler et al., 2021, first described by Kaufman & Rousseeuw, 1990). We then fitted the observations based on their distances into different numbers of clusters using the function 'pam' of the R package 'cluster' (Maechler et al., 2021). With the help of the R package 'NBclust' (Charrad et al., 2014), which suggests the best number of clusters based on 30 indices that apply different distance measures and clustering methods, we decided for a clustering into six PFTs (Figs. S1 and S2). We found that the woody plant species were classified into five evergreen PFTs and one deciduous PFT (PFT 4) (Figs. 3 and S2). The five evergreen PFTs were separated into PFT 1 with a high SLA and leaf nitrogen, PFT 2 with very small and lightweight leaves as well as a low SLA, PFT 3 as nitrogen fixer, PFT 5 with low stomatal conductance and photosynthetic rate, and PFT 6 with a low SLA but with broader, heavier and nitrogen-rich leaves. All regions had species listed within the TRY database that were grouped into each of the PFTs, except for PFT 4 in

Australia, and PFT 6 in Europe/North Africa and South America. Overall, our classification approach approximates many of the morpho-functional characteristics of the species representative of MTEs across the globe.

The resulting six PFTs were then parameterised for ModEST, which requires fixed parameter values for structural, physiological, and reproductive plant traits. As these parameters were not fully covered by the traits used in the cluster analysis, we parameterized them based on additional data resources from TRY and further literature for the plant species that were clustered into the respective PFT (see Table S1). Specifically, we used either the median value for numerical traits or the mode for categorical traits using the available data for all species within the respective PFT.

Table S3 Focal traits for plant functional types (PFTs) classification, their abbreviations, units, data sources, and data coverage per trait (% of data obtained from the particular data source) for all 515 plant species. As the nomenclature in TRY is not always consistent, we merged very similar plant traits. For instance, the trait 'leaf area' included data on the entries 'leaf area', 'leaf area (in case of compound leaves undefined if leaf or leaflet, undefined if petiole and rachis are in- or excluded)', 'leaf area (in case of compound leaves: leaf, petiole included)', and 'leaf area (in case of compound leaves: leaf, undefined if petiole in- or excluded)'.

Plant trait	Abbr.	Unit/Level	Data Sources	Data coverage (%)
Leaf dry mass	Ldm	mg	(Kattge et al., 2011)	36.9
Leaf nitrogen	LNdm	mg*g-1	(Kattge et al., 2011)	67.6
Leaf area	La	mm2	(Kattge et al., 2011)	62.3
Photosynthesis rate per leaf area	Photo	µmol*m-2*s-1	(Kattge et al., 2011)	32.0
Plant height	Ph	m	(Kattge et al., 2011; Köbel et al., 2021; South African National Biodiversity Institute, 2019)	40.2
Stomatal conductance	Stom	mmol*m-2*s-1	(Kattge et al., 2011)	29.5
Specific leaf area	SLA	mm2*mg-1	(Kattge et al., 2011)	71.5
Wood density	Wd	mg*mm-3	(Kattge et al., 2011)	24.7

Plant trait	Abbr.	Unit/Level	Data Sources	Data coverage (%)
Leaf phenology	LPhen	Evergreen vs Deciduous	(California Native Plant Society, 2019; Kattge et al., 2011); Expert knowledge	88.7
N fixation	Nfix	Yes vs No	(California Native Plant Society, 2019; Kattge et al., 2011); Expert knowledge	49.5

59

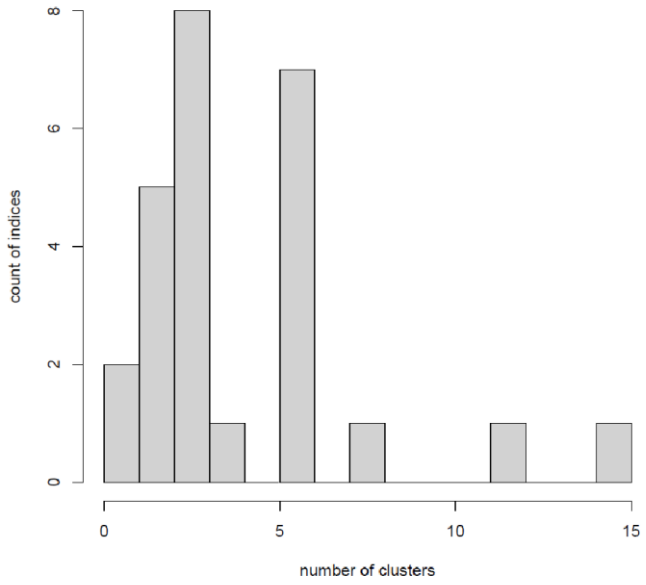

60

61 **Figure S1** Number of indices (y axis) supporting this specific number of clusters (x axis).

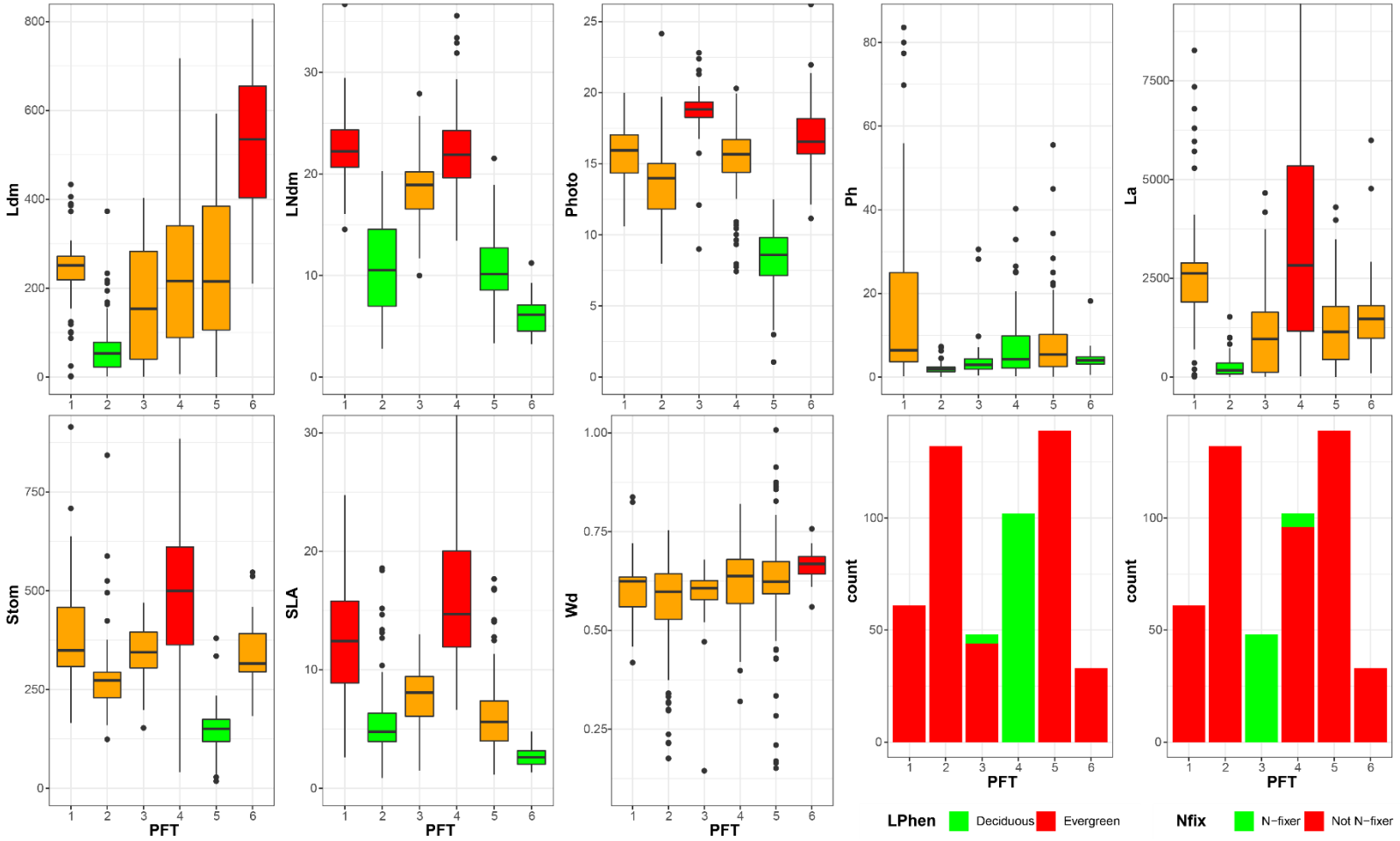

Figure S2 Distributions for each trait (for abbreviations and units see Table S3) for each of the six plant functional types (PFTs) defined for woody Mediterranean-type vegetation by cluster analysis (Fig. 3). For better visualization each trait was further clustered into three levels (green: low value, orange: medium value, red: high value of the trait).

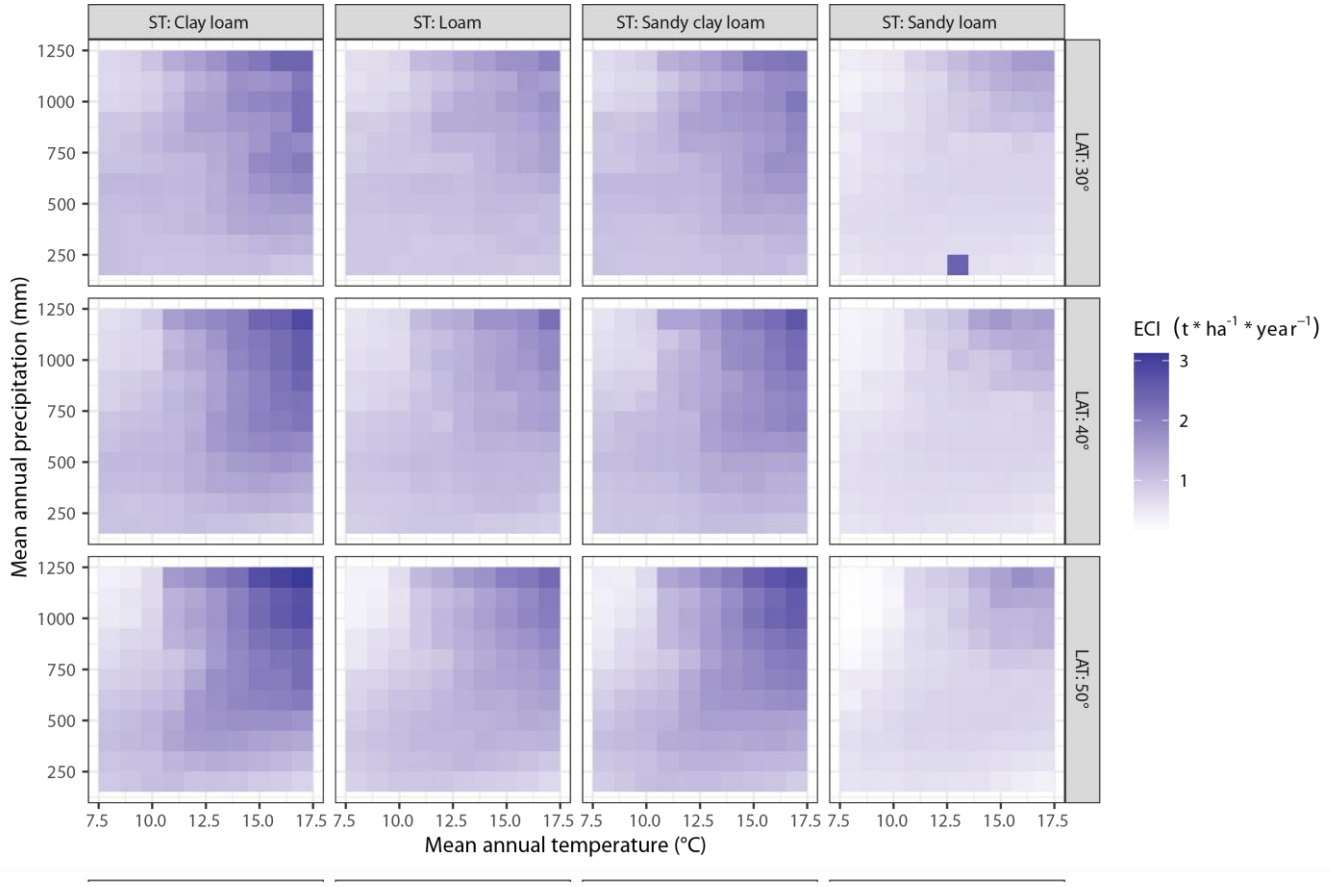

65

66 **Figure S3** Maximised ecosystem carbon increment (ECI) across planted PFT assemblages for each abiotic condition. For each combination (cell) of mean annual precipitation (y axis), mean annual

67 temperature (x axis), soil texture (columns) and solar radiation/latitude (rows), we show maximised ECI across the restoration scenarios. Shown is mean functioning over the simulation years 90 to

68 100 and ten model replicates.

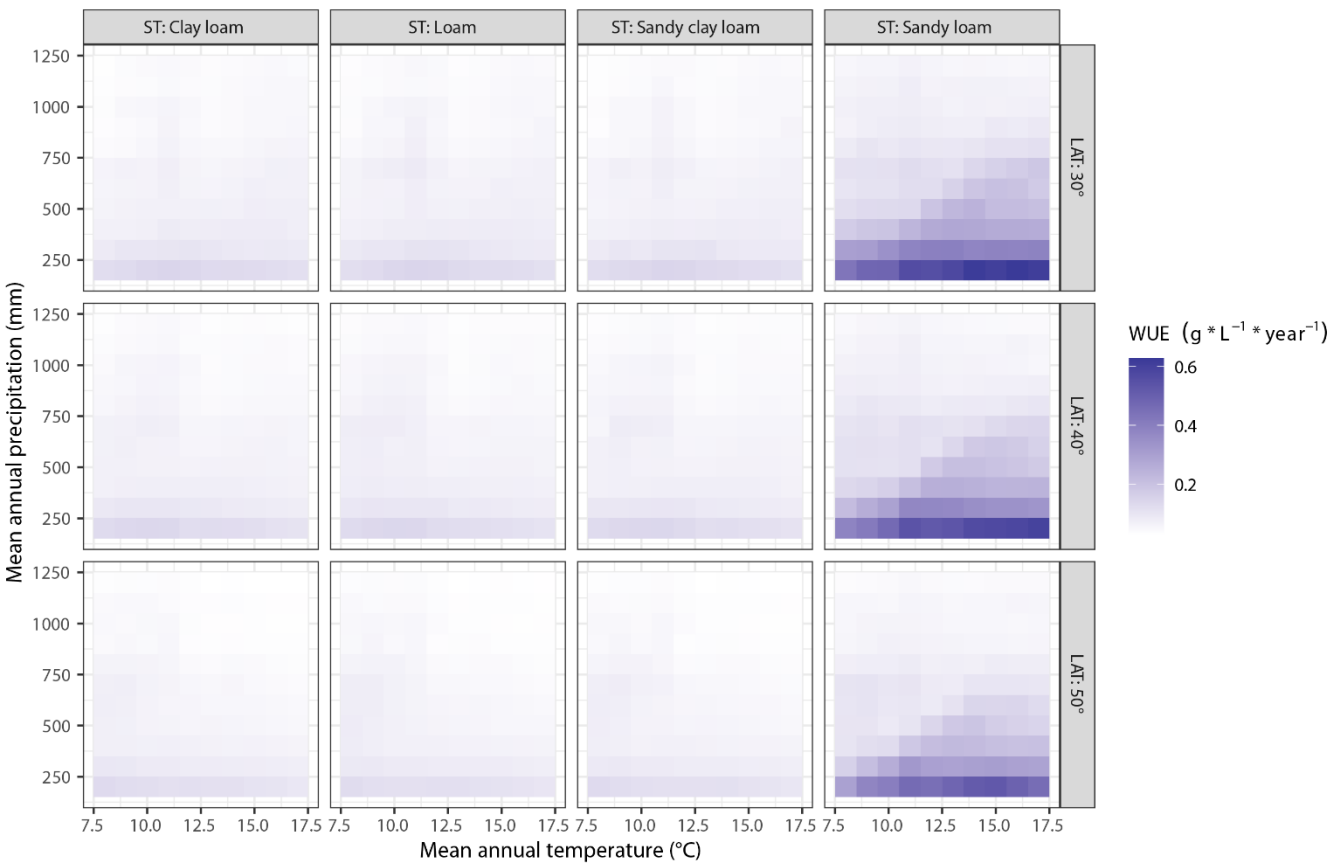

Figure S4 Maximised ecosystem water use efficiency (WUE) across planted PFT assemblages for each abiotic condition. For each combination (cell) of mean annual precipitation (y axis), mean annual temperature (x axis), soil texture (columns) and solar radiation/latitude (rows), we show maximised WUE across the restoration scenarios. Shown is mean functioning over the simulation years 90 to 100 and ten model replicates.

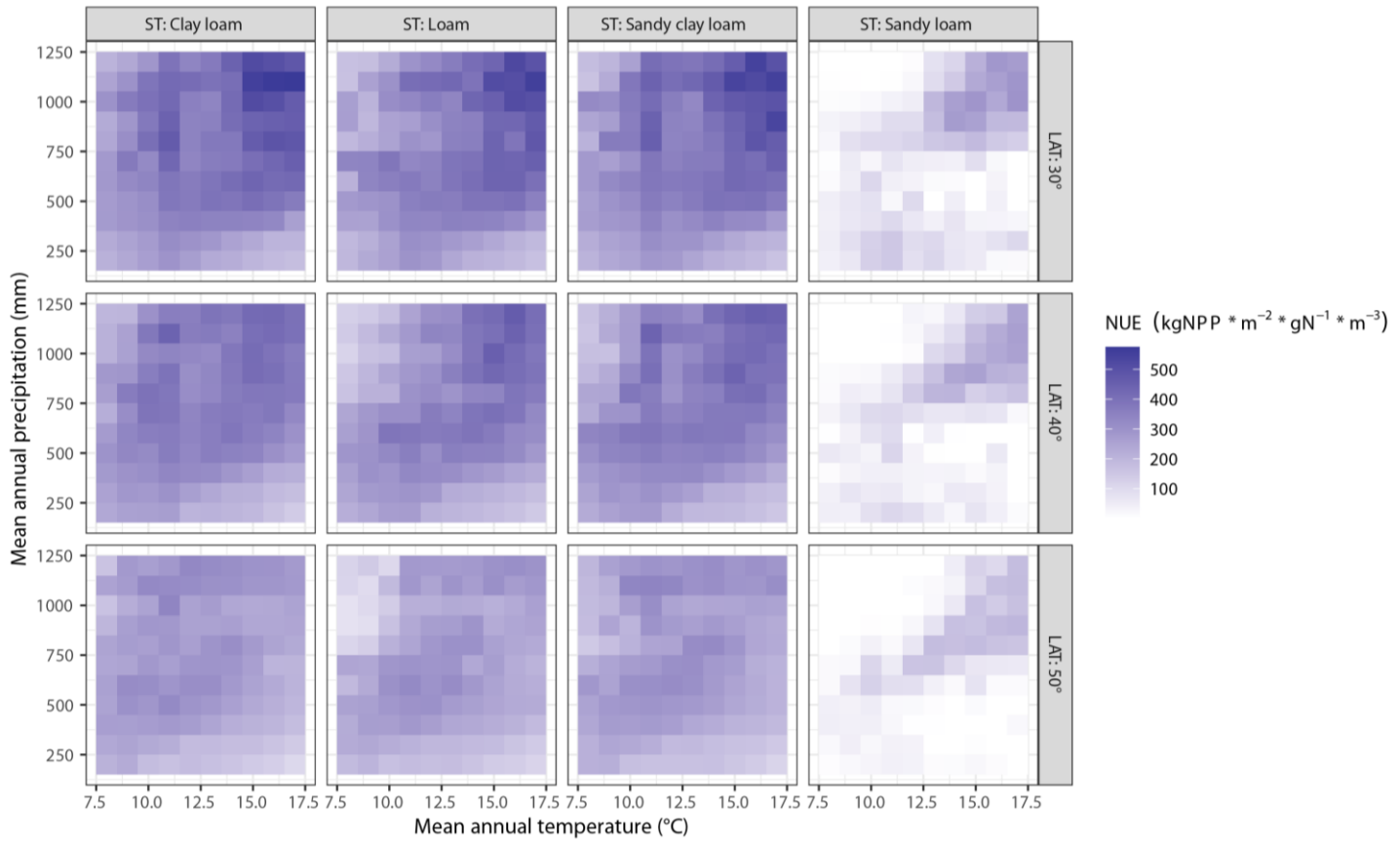

Figure S5 Maximised ecosystem nitrogen use efficiency (NUE) across planted PFT assemblages for each abiotic condition. For each combination (cell) of mean annual precipitation (y axis), mean annual temperature (x axis), soil texture (columns) and solar radiation/latitude (rows), we show maximised NUE across the restoration scenarios. Shown is mean functioning over the simulation years 90 to 100 and ten model replicates.

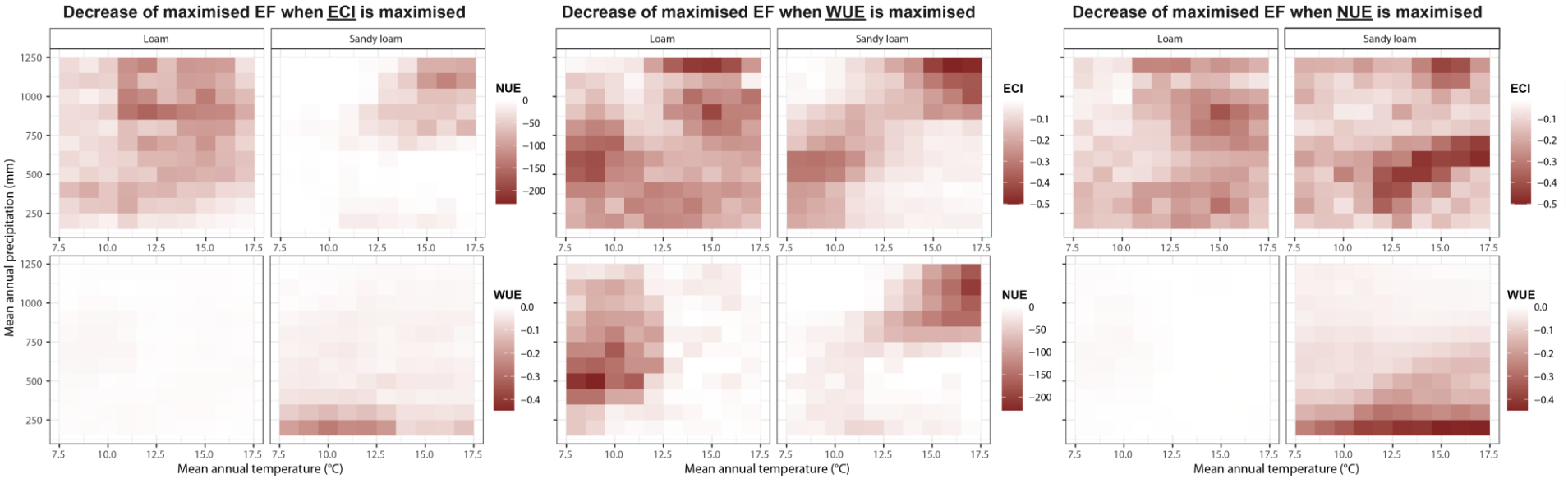

Figure S6 Trade-offs among maximised ecosystem functions (EF) for different abiotic conditions. Ecosystem functions include ecosystem carbon increment (ECI; left, unit: $t \cdot ha^{-1} \cdot year^{-1}$), ecosystem water use efficiency (WUE; centre, unit: $g \cdot L^{-1} \cdot year^{-1}$), and ecosystem nitrogen use efficiency (NUE; right, unit: $kgNPP \cdot m^{-2} \cdot gN^{-1} \cdot m^{-3}$). Abiotic conditions comprise different conditions of mean annual temperature (x axis) and mean annual precipitation (y axis), the two most common soil textures across MTEs (columns: loam and sandy loam), and solar radiation at 40° latitude. The intensity of the red represents the absolute loss of a particular function A compared to its optimal value for this particular abiotic condition, when function B is maximised, where a darker colour indicates a higher loss.

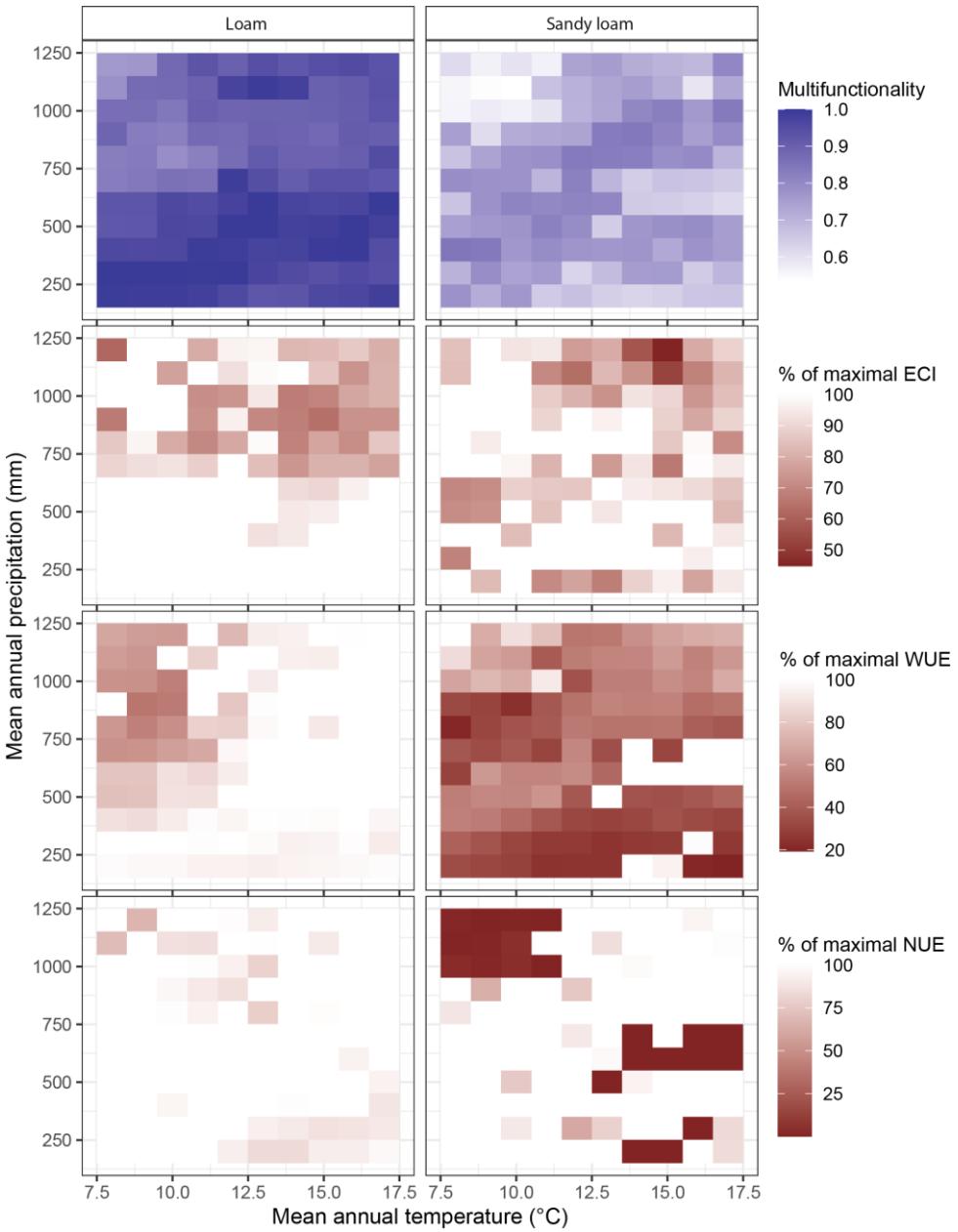

Figure S7 Maximised multifunctionality across planted PFT assemblages for each abiotic condition (top) and loss of provided individual functions compared to when maximised individually (bottom, cp. Figure 4). Shown are mean values over the simulation years 90 to 100 and ten model replicates. Multifunctionality index (0: low, 1: maximal) across all three focal functions is calculated after Fiedler et al. (2021). However, selecting such an index is complex, as it requires prior standardisation of function values to ensure comparability. Different standardisation methods impose varying constraints, and the process often involves weighing individual functions, which can depend heavily on stakeholder priorities (see Fiedler et al. 2021). The results reveal that soil conditions strongly influence the ability to maximise all three functions simultaneously. Under sandier conditions, greater compromises are required, particularly in maximising water-use efficiency.

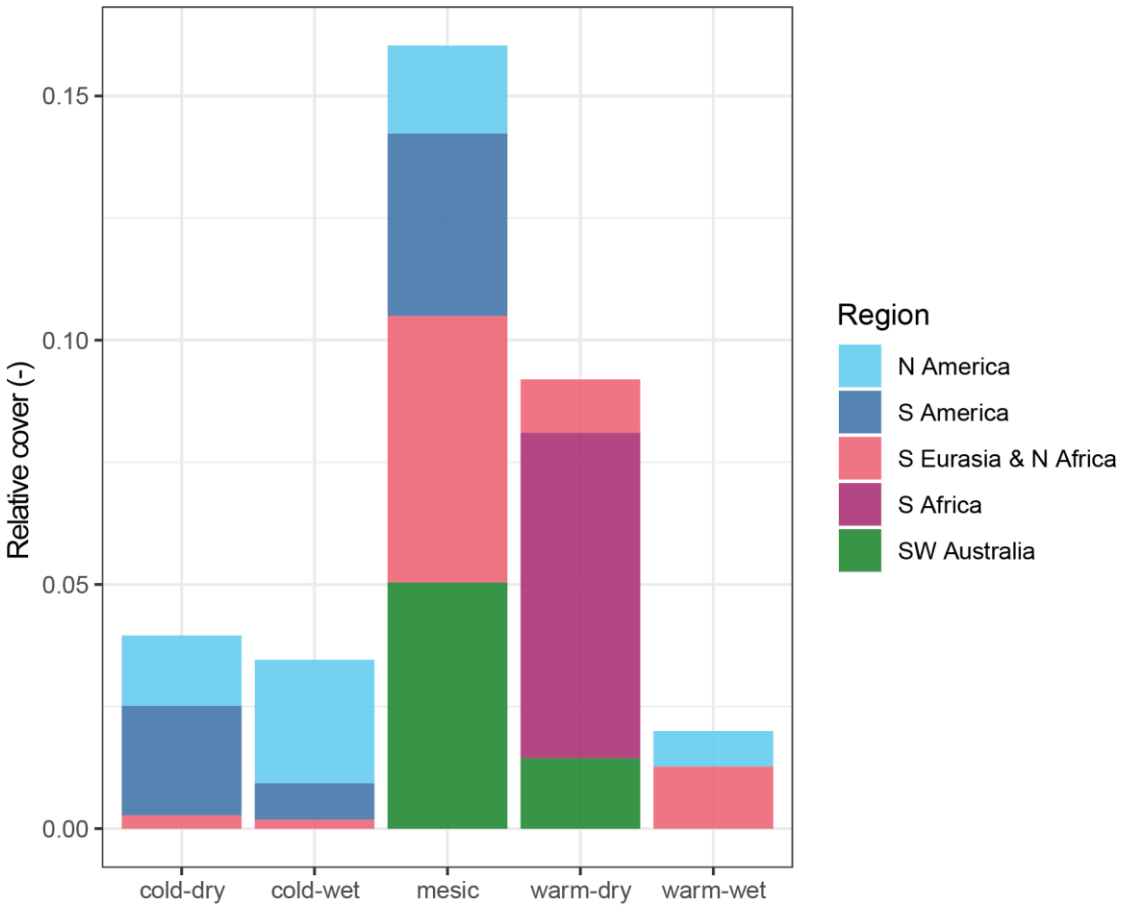

Figure S8 Relative cover (pixel counts divided by total pixel of the MTE region) of each MTE region for each focal abiotic condition. Selected climatic conditions are (compare with coloured bordered squares in Figure 4) 'cold-wet' with MAP = 1100 mm and MAT = 9°C, 'cold-dry' with MAP = 300 mm and MAT = 9°C, 'mesic' with MAP = 700 mm and MAT = 13°C, 'warm-wet' with MAP = 1100 mm and MAT = 16°C, and 'warm-dry' with MAP = 300 mm and MAT = 16°C. We counted the pixels that were at least in a ± 10% range of the respective condition.

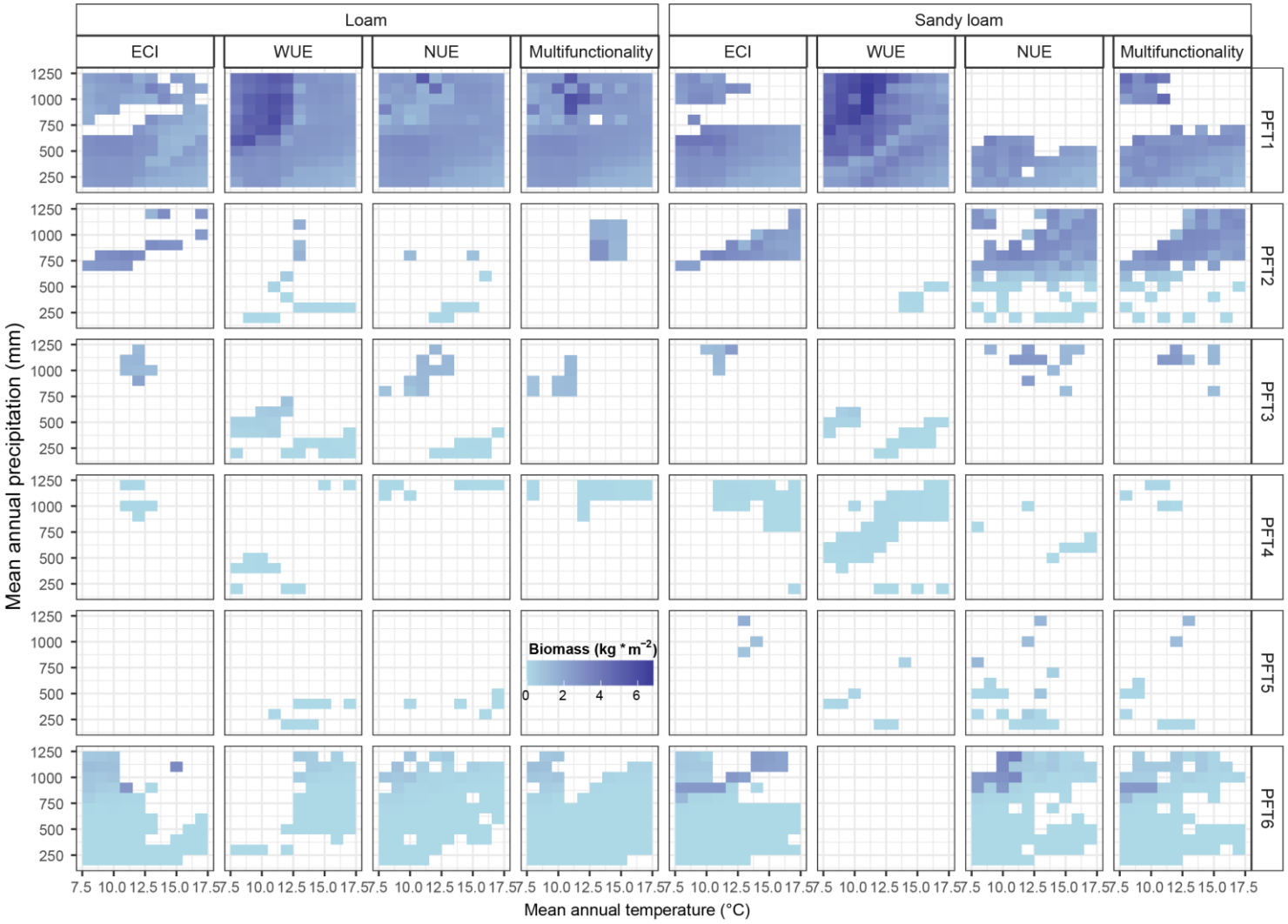

Figure S9 Biomass per PFT of the restoration scenarios that provided maximised individual ecosystem functions or multifunctionality for different abiotic conditions. Mean PFT's biomass (between 90 and 100 years, 10 model replicates) is given for each maximised ecosystem function or maximised multifunctionality (columns) and for different mean annual precipitation (y axis), mean annual temperature (x axis) with soil textures 'loam' and 'sandy loam' and solar radiation at 40° latitude. Multifunctionality across all three focal functions was calculated as described in Fiedler et al. (2021). See results on maximised multifunctionality across abiotic contexts in Fig. S7.

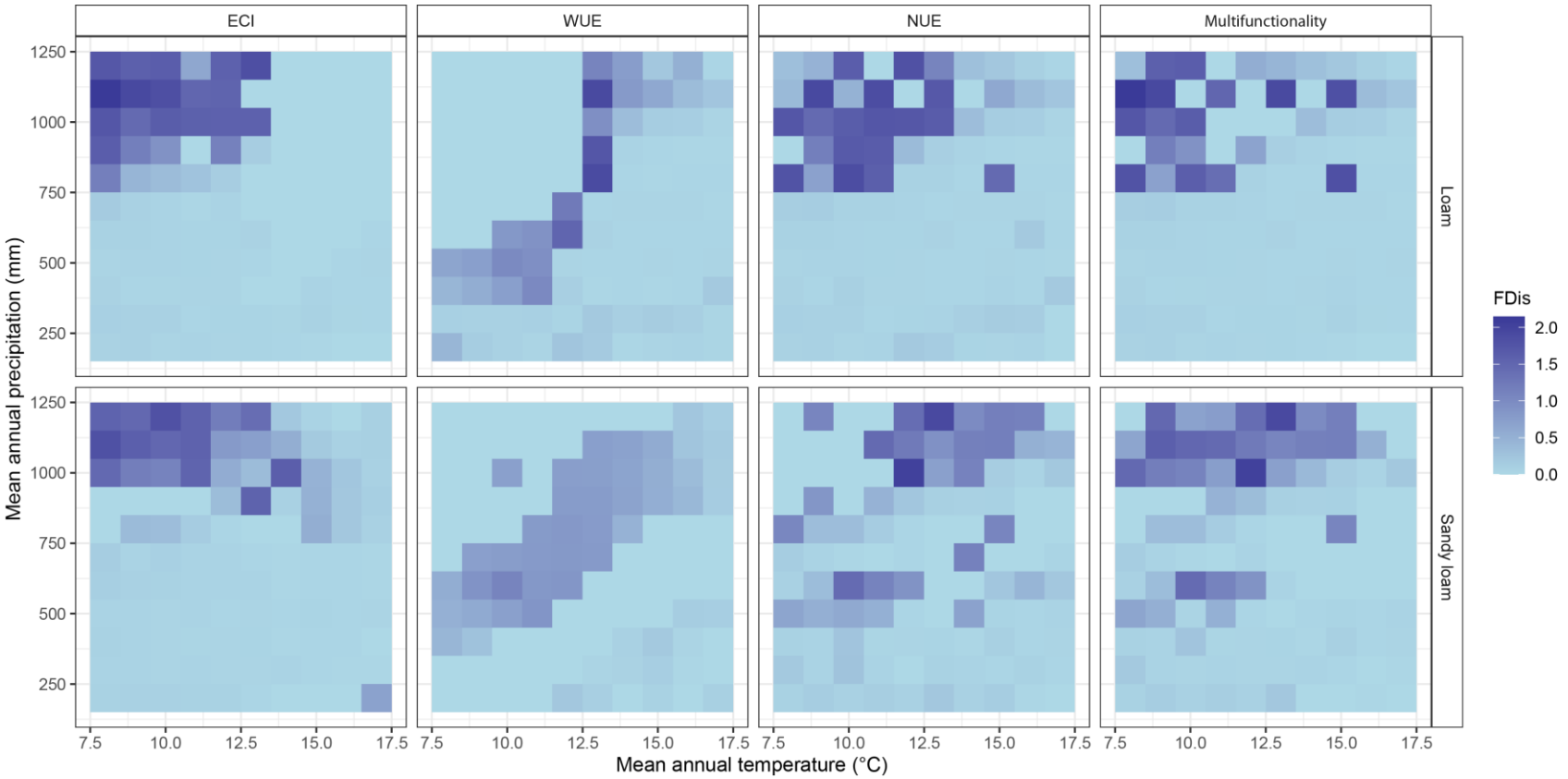

Figure S10 Functional dispersion (FDis) of the restoration scenarios that provided maximised individual ecosystem functions or multifunctionality for different abiotic conditions. Mean FDis (between 90 and 100 years, 10 model replicates) is given for each maximised ecosystem function or maximised multifunctionality (columns) and for different mean annual precipitation (y axis), mean annual temperature (x axis) with soil textures 'loam' and 'sandy loam' (rows) and solar radiation at 40° latitude. FDis was calculated as described in Figure S4.1 of Fiedler et al. (2021).

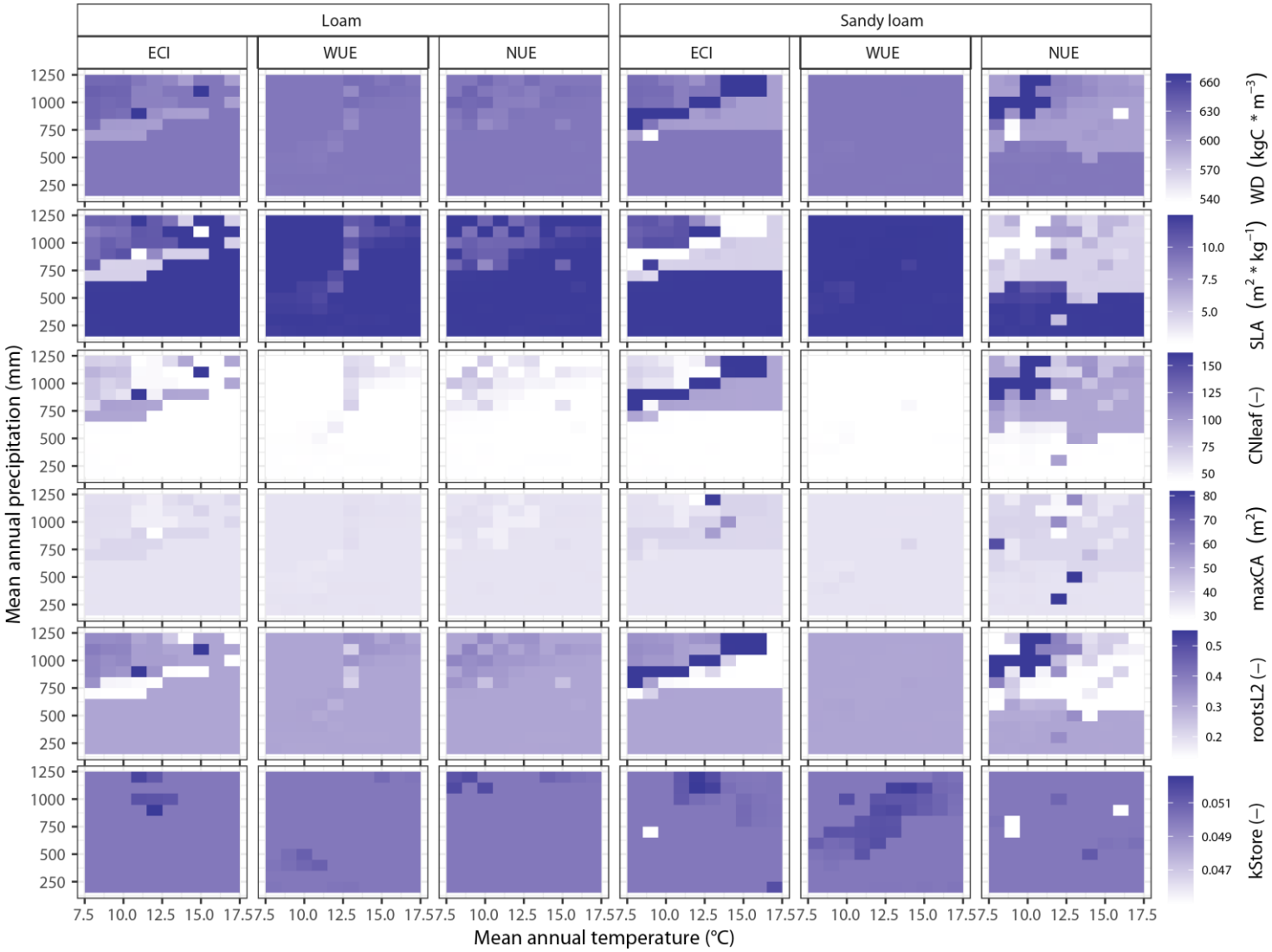

Figure S11 Community weighted mean (CWM) plant traits of PFT assemblages that provide maximised ecosystem functioning for different environmental settings. CWM is given for each ecosystem function (columns) and for different mean annual precipitation (y axis), mean annual temperature (x axis) for the two most common soil textures across Mediterranean-type ecosystems (loam and sandy loam) and solar radiation at 40° latitude. For trait abbreviations, refer to Table S1.

Supporting Information References

Bartlett, M. K., Scoffoni, C., & Sack, L. (2012). The determinants of leaf turgor loss point and prediction of drought tolerance of species and biomes: A global meta-analysis. Ecology Letters, 15(5), 393–405. https://doi.org/10.1111/j.1461-0248.2012.01751.x

California Native Plant Society. (2019, May). https://calscape.org/.

Charrad, M., Ghazzali, N., Boiteau, V., & Niknafs, A. (2014). {NbClust}: An {R} Package for Determining the Relevant Number of Clusters in a Data Set. Journal of Statistical Software, 61(6), 1–36. http://www.jstatsoft.org/v61/i06/

Dentener, F., Drevet, J., Lamarque, J. F., Bey, I., Eickhout, B., Fiore, A. M., Hauglustaine, D., Horowitz, L. W., Krol, M., Kulshrestha, U. C., Lawrence, M., Galy-Lacaux, C., Rast, S., Shindell, D., Stevenson, D., Van Noije, T., Atherton, C., Bell, N., Bergman, D., … Wild, O. (2006). Nitrogen and sulfur deposition on regional and global scales: A multimodel evaluation. Global Biogeochemical Cycles, 20(4). https://doi.org/10.1029/2005GB002672

Díaz Barradas, M. C., Zunzunegui, M., Tirado, R., Ain-Lhout, F., & García Novo, F. (1999). Plant functional types and ecosystem function in Mediterranean shrubland. Journal of Vegetation Science, 10(5), 709–716. https://doi.org/10.2307/3237085

Enright, N. J., Fontaine, J. B., Lamont, B. B., Miller, B. P., & Westcott, V. C. (2014). Resistance and resilience to changing climate and fire regime depend on plant functional traits. Journal of Ecology, 102(6), 1572–1581. https://doi.org/10.1111/1365-2745.12306

Kattge, J., Bönisch, G., Díaz, S., Lavorel, S., Prentice, I. C., Leadley, P., Tautenhahn, S., Werner, G. D. A., Aakala, T., Abedi, M., Acosta, A. T. R., Adamidis, G. C., Adamson, K., Aiba, M., Albert, C. H., Alcántara, J. M., Alcázar C, C., Aleixo, I., Ali, H., … Wirth, C. (2020). TRY plant trait database – enhanced coverage and open access. Global Change Biology, 26(1), 119–188. https://doi.org/10.1111/gcb.14904

Kattge, J., Díaz, S., Lavorel, S., Prentice, I. C., Leadley, P., Bönisch, G., Garnier, E., Westoby, M., Reich, P. B., Wright, I. J., Cornelissen, J. H. C., Violle, C., Harrison, S. P., Van Bodegom, P. M., Reichstein, M., Enquist, B. J., Soudzilovskaia, N. A., Ackerly, D. D., Anand, M., … Wirth, C. (2011). TRY - a global database of plant traits. Global Change Biology, 17(9), 2905–2935. https://doi.org/10.1111/j.1365-2486.2011.02451.x

Kaufman, L., & Rousseeuw, P. J. (1990). Finding Groups in Data An Introduction to Cluster Analysis.

Köbel, M., Listopad, C. M. C. S., Príncipe, A., Nunes, A., & Branquinho, C. (2021). Temporary grazing exclusion as a passive restoration strategy in a dryland woodland: Effects over time on tree regeneration and on the shrub community. Forest Ecology and Management, 483, 118732. https://doi.org/10.1016/j.foreco.2020.118732

Köppen, W. (1900). Versuch einer Klassifikation der Klimate, vorzugsweise nach ihren Beziehungen zur Pflanzenwelt on JSTOR. Geographische Zeitschrift, 6(11), 593–611. https://www.jstor.org/stable/27803924

Koniak, G., Noy-Meir, I., & Perevolotsky, A. (2009). Estimating multiple benefits from vegetation in mediterranean ecosystems. Biodiversity and Conservation, 18(13), 3483–3501. https://doi.org/10.1007/s10531-009-9656-9

Koniak, G., Noy-Meir, I., & Perevolotsky, A. (2011). Modelling dynamics of ecosystem services basket in Mediterranean landscapes: a tool for rational management. Landscape Ecology, 26(1), 109–124. https://doi.org/10.1007/s10980-010-9540-8

Kottek, M., Grieser, J., Beck, C., Rudolf, B., & Rubel, F. (2006). World Map of the Köppen-Geiger climate classification updated. Meteorologische Zeitschrift, 15(3), 259–263. https://doi.org/10.1127/0941-2948/2006/0130

Maechler, M., Rousseeuw, P., Struyf, A., Hubert, M., & Hornik, K. (2021). cluster: Cluster Analysis Basics and Extensions. https://CRAN.R-project.org/package=cluster

Peel, M. C., Finlayson, B. L., & McMahon, T. A. (2007). Updated world map of the Köppen-Geiger climate classification. Hydrology and Earth System Sciences, 11(5), 1633–1644. https://doi.org/10.5194/hess-11-1633-2007

Perring, M. P., Standish, R. J., Hulvey, K. B., Lach, L., Morald, T. K., Parsons, R., Didham, R. K., & Hobbs, R. J. (2012). The Ridgefield Multiple Ecosystem Services Experiment: Can restoration of former agricultural land achieve multiple outcomes? Agriculture, Ecosystems & Environment, 163, 14–27. https://doi.org/10.1016/j.agee.2012.02.016

Rawls, W. J., Ahuja, L. R., Brakensiek, D. L., & Shirmohammadi, A. (1992). Infiltration and soil water movement. In D. R. Maidment (Ed.), Handbook of Hydrology (1st ed.). McGraw-Hill Professional.

Schaphoff, S., von Bloh, W., Rammig, A., Thonicke, K., Biemans, H., Forkel, M., Gerten, D., Heinke, J., Jägermeyr, J., Knauer, J., Langerwisch, F., Lucht, W., Müller, C., Rolinski, S., & Waha, K. (2018). LPJmL4 – a dynamic global vegetation model with managed land – Part 1: Model description. Geoscientific Model Development, 11(4), 1343–1375. https://doi.org/10.5194/gmd-11-1343-2018

Sitch, S., Prentice, I. C., Smith, B., Cramer, W., Kaplan, J. O., Lucht, W., Sykes, M., Thonicke, K., & Venevsky, S. (2000). LPJ - A coupled model of vegetation dynamics and the terrestrial carbon cycle. The Role of Vegetation Dynamics in the Control of Atmospheric CO2 Content, Ph.D. Thesis. http://infoscience.epfl.ch/record/117482

Sitch, S., Smith, B., Prentice, I. C., Arneth, a., Bondeau, a., Cramer, W., Kaplan, J. O., Levis, S., Lucht, W., Sykes, M. T., Thonicke, K., & Venevsky, S. (2003). Evaluation of ecosystem dynamics, plant geography and terrestrial carbon cycling in the LPJ dynamic global vegetation model. Global Change Biology, 9(2), 161–185. https://doi.org/10.1046/j.1365-2486.2003.00569.x

Smith, B., Wårlind, D., Arneth, A., Hickler, T., Leadley, P., Siltberg, J., & Zaehle, S. (2014). Implications of incorporating N cycling and N limitations on primary production in an individual-based dynamic vegetation model. Biogeosciences, 11(7), 2027–2054. https://doi.org/10.5194/bg-11-2027-2014

South African National Biodiversity Institute. (2019, May). http://pza.sanbi.org/.

Stekhoven, D. J., & Buhlmann, P. (2012). MissForest--non-parametric missing value imputation for mixed-type data. Bioinformatics, 28(1), 112–118. https://doi.org/10.1093/bioinformatics/btr597

Thomson, F. J., Moles, A. T., Auld, T. D., & Kingsford, R. T. (2011). Seed dispersal distance is more strongly correlated with plant height than with seed mass. Journal of Ecology, 99(6), 1299–1307. https://doi.org/10.1111/j.1365-2745.2011.01867.x

Tietjen, B., Zehe, E., & Jeltsch, F. (2009). Simulating plant water availability in dry lands under climate change: A generic model of two soil layers. Water Resources Research, 45(1), 1–14. https://doi.org/10.1029/2007WR006589

USDA. (2020). Soil Texture Calculator. https://www.nrcs.usda.gov/wps/portal/nrcs/detail/soils/survey/?cid=nrcs142p2_054167

W. J. Rawls, D. Gimenez, & R. Grossman. (1998). Use of soil texture, bulk density, and slope of the water retention curve to predict saturated hydraulic conductivity. Transactions of the ASAE, 41(4), 983–988. https://doi.org/10.13031/2013.1727